

Fast Layout-Oblivious Tensor-Matrix Multiplication with BLAS

Cem Savaş Başsoy

Hamburg University of Technology, Schwarzenbergstrasse 95, Germany,
cem.bassoy@gmail.com

Abstract. The tensor-matrix multiplication is a basic tensor operation required by various tensor methods such as the ALS and the HOSVD. This paper presents flexible high-performance algorithms that compute the tensor-matrix product according to the Loops-over-GEMM (LoG) approach. Our algorithms can process dense tensors with any linear tensor layout, arbitrary tensor order and dimensions all of which can be runtime variable. We discuss different tensor slicing methods with parallelization strategies and propose six algorithm versions that call BLAS with subtensors or tensor slices. Their performance is quantified on a set of tensors with various shapes and tensor orders. Our best performing version attains a median performance of 1.37 double precision Tflops on an Intel Xeon Gold 6248R processor using Intel’s MKL. We show that the tensor layout does not affect the performance significantly. Our fastest implementation is on average at least 14.05% and up to 3.79x faster than other state-of-the-art approaches and actively developed libraries like Libtorch and Eigen.

1 Introduction

Tensor computations are found in many scientific fields such as computational neuroscience, pattern recognition, signal processing and data mining [4, 11]. These computations use basic tensor operations as building blocks for decomposing and analyzing multidimensional data which are represented by tensors [5, 6]. Tensor contractions are an important subset of basic operations that need to be fast for efficiently solving tensor methods.

There are three main approaches for implementing tensor contractions. The Transpose-Transpose-GEMM-Transpose (TTGT) approach reorganizes (flattens) tensors in order to perform a tensor contraction using optimized General Matrix Multiplication (GEMM) implementations [1, 15]. Implementations of the GEMM-like Tensor-Tensor multiplication (GETT) method have macro-kernels that are similar to the ones used in fast GEMM implementations [9, 16]. The third method is the Loops-over-GEMM (LoG) approach in which BLAS are utilized with multiple tensor slices or subtensors if possible [2, 7, 10, 14]. Implementations of the LoG and TTGT approaches are in general easier to maintain and faster to port than GETT implementations which might need to adapt vector instructions or blocking parameters according to a processor’s microarchitecture.

In this work, we present high-performance algorithms for the tensor-matrix multiplication which is used in many numerical methods such as the alternating least squares method [5, 6]. It is a compute-bound tensor operation and has the same arithmetic intensity as a matrix-matrix multiplication which can almost reach the practical peak performance of a computing machine.

To our best knowledge, we are the first to combine the LoG approach described in [2, 13] for tensor-vector multiplications with the findings on tensor slicing for the tensor-matrix multiplication in [7]. Our proposed algorithms support dense tensors with any order, dimensions and any linear tensor layout including the first- and the last-order storage formats for any contraction mode all of which can be runtime variable. They compute the tensor-matrix product in parallel using efficient GEMM or batched GEMM without transposing or flattening tensors. Despite their high performance, all algorithms are layout-oblivious and provide without tuning a sustained performance independent of the tensor layout.

Moreover, every proposed algorithm can be implemented with less than 150 lines of C++ code where the algorithmic complexity is reduced by the BLAS implementation and the corresponding selection of subtensors or tensor slices. We have provided an open and free reference C++ implementation of all algorithms and a python interface for convenience. While Intel’s MKL is used for our benchmarks, the user is free to select any other library that provides the BLAS interface.

The following analysis quantifies the impact of the tensor layout, the tensor slicing method and parallel execution of slice-matrix multiplications with varying contraction modes. The runtime measurements of our implementations are compared with state-of-the-art approaches discussed in [9, 12, 16] including Libtorch and Eigen. In summary, the main findings of our work are:

- A tensor-matrix multiplication can be implemented by an in-place algorithm with 1 GEMV and 7 GEMM calls, supporting all combinations of contraction mode, tensor order and dimensions for any linear tensor layout.
- Our fastest algorithm with tensor slices is on average 17% faster than Intel’s batched GEMM implementation when the contraction and leading dimensions of the tensors are greater than 256.
- The proposed algorithms are layout-oblivious. Their performance does not vary significantly for different tensor layouts if the contraction conditions remain the same.
- Our fastest algorithm computes the tensor-matrix multiplication on average, by at least 14.05% and up to a factor of 3.79 faster than other state-of-the-art library implementations, including LibTorch and Eigen.

The remainder of the paper is organized as follows. Section 2 presents related work. Section 3 introduces some notation on tensors and defines the tensor-matrix multiplication. Algorithm design and methods for slicing and parallel execution are discussed in Section 4. Section 5 describes the test setup. Benchmark results are presented in Section 6. Conclusions are drawn in Section 7.

2 Related Work

The authors of [16] present a tensor-contraction generator TCCG and the GETT approach for dense tensor contractions that is inspired from the design of a high-performance GEMM. Their unified code generator selects implementations from generated GETT, LoG and TTGT candidates. Their findings show that among 48 different contractions 15% of LoG-based implementations are the fastest.

The author presents in [9] a runtime flexible tensor contraction library that uses GETT approach as well. He describes block-scatter-matrix algorithm which uses a special layout for the tensor contraction. The proposed algorithm yields results that feature a similar runtime behavior to those presented in [16].

The work in [7] introduces InTensLi, a framework that generates in-place tensor-matrix multiplication according to the LOG approach. The authors discuss optimization and tuning techniques for slicing and parallelizing the operation. With optimized tuning parameters, they report a speedup of up to 4x over the TTGT-based MATLAB tensor toolbox library discussed in [1].

In [2], the author presents LoG-based algorithms that compute the tensor-vector product. They support dense tensors with linear tensor layouts, arbitrary dimensions and tensor order. The presented approach is to divide into eight cases calling GEMV and DOT. He reports average speedups of 6.1x and 4.0x compared to implementations that use the TTGT and GETT approach, respectively.

The authors in [13] propose morton-ordered blocked layout for a mode-oblivious performance of the tensor-vector multiplication. Their algorithm iterate over blocked tensors and perform tensor-vector multiplications on blocked tensors. They are able to achieve high performance and mode-oblivious computations.

3 Background

Notation An order- p tensor is a p -dimensional array [8] where tensor elements are contiguously stored in memory. We write a , \mathbf{a} , \mathbf{A} and $\underline{\mathbf{A}}$ in order to denote scalars, vectors, matrices and tensors. If not otherwise mentioned, we assume $\underline{\mathbf{A}}$ to have a tensor order p with $p > 2$. The p -tuple \mathbf{n} with $\mathbf{n} = (n_1, n_2, \dots, n_p)$ will be referred to as a dimension tuple with $n_r > 1$. We will use round brackets $\underline{\mathbf{A}}(i_1, i_2, \dots, i_p)$ or $\underline{\mathbf{A}}(\mathbf{i})$ to denote a tensor element where $\mathbf{i} = (i_1, i_2, \dots, i_p)$ is a multi-index. A subtensor is denoted by $\underline{\mathbf{A}}'$ and references elements of a tensor $\underline{\mathbf{A}}$. They are specified by a selection grid consisting of p index ranges. The index range in this work shall either address all indices of a given mode or a by a single index i_r with $1 \leq r \leq p$. Elements n'_r of a subtensor's dimension tuple \mathbf{n}' are $n'_r = n_r$ if all indices of mode r are selected or $n'_r = 1$. We will annotate subtensors using only their non-unit modes such as $\underline{\mathbf{A}}'_{u,v,w}$ where $n_u > 1, n_v > 1$ and $n_w > 1$ and $1 \leq u \neq v \neq w \leq p$. The remaining single indices of a selection grid correspond to the loop induction variables of the following algorithms. A subtensor is called a slice $\underline{\mathbf{A}}'_{u,v}$ if the full range selection of $\underline{\mathbf{A}}$ occurs with only two modes. A fiber $\underline{\mathbf{A}}'_u$ is a tensor slice with only one dimension greater than 1.

Linear Tensor Layouts We use a layout tuple $\boldsymbol{\pi} \in \mathbb{N}^p$ to encode all linear tensor layouts including the first-order or last-order layout. They contain permuted tensor modes whose priority is given by their index. The general k -order tensor layout for an order- p tensor is given by the layout tuple $\boldsymbol{\pi}$ with $\pi_r = k - r + 1$ for $1 < r \leq k$ and r for $k < r \leq p$. For instance, the first- and last-order storage formats are given by $\boldsymbol{\pi}_F = (1, 2, \dots, p)$ and $\boldsymbol{\pi}_L = (p, p-1, \dots, 1)$. An inverse layout tuple $\boldsymbol{\pi}^{-1}$ is defined by $\boldsymbol{\pi}^{-1}(\boldsymbol{\pi}(k)) = k$. Given a layout tuple $\boldsymbol{\pi}$ with p modes, the π_r -th element of a stride tuple is given by $w_{\pi_r} = \prod_{k=1}^{r-1} n_{\pi_k}$ for $1 < r \leq p$ and $w_{\pi_1} = 1$. Tensor elements of the π_1 -th mode are contiguously stored in memory. The location of tensor elements is determined by the tensor layout and the layout function. For a given tensor layout and stride tuple, a layout function $\lambda_{\mathbf{w}}$ maps a multi-index to a scalar index with $\lambda_{\mathbf{w}}(\mathbf{i}) = \sum_{r=1}^p w_r(i_r - 1)$, see [3, 13].

Non-Modifying Flattening and Reshaping The flattening operation $\varphi_{r,q}$ transforms an order- p tensor $\underline{\mathbf{A}}$ to another order- p' view $\underline{\mathbf{B}}$ that has different a shape \mathbf{m} and layout $\boldsymbol{\tau}$ tuple of length p' with $p' = p - q + r$ and $1 \leq r < q \leq p$. It is related to the tensor unfolding operation as defined in [5, p.459] but neither changes the element ordering nor copies tensor elements. Given a layout tuple $\boldsymbol{\pi}$ of $\underline{\mathbf{A}}$, the flattening operation $\varphi_{r,q}$ is defined for contiguous modes $\hat{\boldsymbol{\pi}} = (\pi_r, \pi_{r+1}, \dots, \pi_q)$ of $\boldsymbol{\pi}$. Let $j = 0$ if $k \leq r$ and $j = q - r$ otherwise for $1 \leq k \leq p'$. Then the resulting layout tuple $\boldsymbol{\tau} = (\tau_1, \dots, \tau_{p'})$ of $\underline{\mathbf{B}}$ is given by $\tau_r = \min(\pi_{r,q})$ and $\tau_k = \pi_{k+j} + s_k$ if $k \neq r$ where $s_k = |\{\pi_i \mid \pi_{k+j} > \pi_i \wedge \pi_i \neq \min(\hat{\boldsymbol{\pi}}) \wedge r \leq i \leq p\}|$. Elements of the shape tuple \mathbf{m} are defined by $m_{\tau_r} = \prod_{k=r}^q n_{\pi_k}$ and $m_{\tau_k} = n_{\pi_{k+j}}$ if $k \neq r$. Reshaping ρ transforms an order- p tensor $\underline{\mathbf{A}}$ to another order- p tensor $\underline{\mathbf{B}}$ with the shape tuple \mathbf{m} and layout tuple $\boldsymbol{\tau}$ tuples, both of length p . In this work, it permutes the shape and layout tuple simultaneously without changing the element ordering and without copying tensor elements. The operation ρ is defined by a permutation tuple $\boldsymbol{\rho} = (\rho_1, \dots, \rho_p)$ that defines elements of \mathbf{m} and $\boldsymbol{\tau}$ with $m_r = n_{\rho_r}$ and $\tau_r = \pi_{\rho_r}$, respectively.

Tensor-Matrix Multiplication Let $\underline{\mathbf{A}}$ and $\underline{\mathbf{C}}$ be order- p tensors with shapes $\mathbf{n}_a = (n_1, \dots, n_q, \dots, n_p)$ and $\mathbf{n}_c = (n_1, \dots, n_{q-1}, m, n_{q+1}, \dots, n_p)$. Let \mathbf{B} be a matrix of shape $\mathbf{n}_b = (m, n_q)$. A mode- q tensor-matrix product is denoted by $\underline{\mathbf{C}} = \underline{\mathbf{A}} \times_q \mathbf{B}$. An element of $\underline{\mathbf{C}}$ is defined by

$$\underline{\mathbf{C}}(i_1, \dots, i_{q-1}, j, i_{q+1}, \dots, i_p) = \sum_{i_q=1}^{n_q} \underline{\mathbf{A}}(i_1, \dots, i_q, \dots, i_p) \cdot \mathbf{B}(j, i_q) \quad (1)$$

with $1 \leq i_r \leq n_r$ and $1 \leq j \leq m$, see [5, 7]. Mode q is called the *contraction mode* with $1 \leq q \leq p$. The tensor-matrix multiplication generalizes the computational aspect of the two-dimensional case $\mathbf{C} = \mathbf{B} \cdot \mathbf{A}$ if $p = 2$ and $q = 1$. Its arithmetic intensity is equal to that of a matrix-matrix multiplication and is not memory-bound. In the following, we assume that the tensors $\underline{\mathbf{A}}$ and $\underline{\mathbf{C}}$ have the same tensor layout $\boldsymbol{\pi}$. Elements of matrix \mathbf{B} can be stored either in the column-major

or row-major format. Without loss of generality, we assume \mathbf{B} to have the row-major storage format in this work. Also note that all of the following analysis is valid, if the matrix indices j and i_q are swapped.

4 Algorithm Design

4.1 Baseline Algorithm with Contiguous Memory Access

The sequential algorithm for Eq. 1 can be implemented with a single C++ function. It consists of nested recursion with a control flow that is akin to algorithm 1 in [3] consisting of two `if` statements with an `else` branch. The latter consists of two loops that compute a fiber-matrix product. The outer loop iterates with j over the dimension m of \mathbf{C} and \mathbf{B} . The inner loop iterates with i_q over the dimension n_q of \mathbf{A} and \mathbf{B} computing an inner product. This version accesses elements of \mathbf{A} and \mathbf{C} non-contiguously whenever $\pi_1 \neq q$. Matrix \mathbf{B} is contiguously accessed if i_q or j is incremented with unit-strides depending on the storage format of \mathbf{B} .

A more efficient solution is to access tensor elements according to the tensor layout. Our baseline algorithm is given in Algorithm 1 which contiguously accesses memory for $\pi_1 \neq q$ and $p > 1$. Each recursion level adjusts only one multi-index element i_{π_r} with a stride w_{π_r} in line 5. With increasing recursion level and decreasing r , indices are incremented with smaller strides as $w_{\pi_r} \leq w_{\pi_{r+1}}$. The second `if` statement in line 4 allows the mode- π_1 loop with index i_{π_1} and the minimum stride w_{π_1} to be included in the base case. The latter now contains three loops performing a slice-matrix multiplication. The inner-most loop increments i_{π_1} and contiguously accesses tensor elements of \mathbf{A} and \mathbf{C} . The second loop increments i_q with which elements of \mathbf{B} are contiguously accessed if \mathbf{B} is stored in the row-major format. The third loop increments j and could be placed as the second loop if \mathbf{B} is stored in the column-major format.

While spatial data locality is improved by adjusting the loop ordering, the temporal data locality of tensors \mathbf{A} and \mathbf{C} differ. Note that slice $\mathbf{A}'_{\pi_1, q}$, fiber \mathbf{C}'_{π_1} and element $\mathbf{B}(j, i_q)$ are accessed m , n_q and n_{π_1} times, respectively. While the specified fiber of \mathbf{C} can fit into first or second level cache, slice elements of \mathbf{A} are unlikely to fit in the local caches if the slice size $n_{\pi_1} \times n_q$ is large leading to higher cache misses and suboptimal performance. Instead of optimizing for better temporal data locality, we use existing high-performance BLAS implementations for the base case.

4.2 BLAS-based Algorithms with Tensor Slices

Algorithm 1 is the starting point for the BLAS-based algorithm which computes the tensor-matrix product with a `gemm` routine. Besides the illustrated algorithm, we have identified seven other cases where a single `gemm` call suffices to compute the tensor-matrix product even if the tensor order $p > 2$. In summary, there are eight cases with a single `gemm` call using different arguments which are listed in table 1. The list of `gemm` calls supports all linear tensor layout and has no

```

1 tensor_times_matrix(A, B, C, n, i, m, q, q̂, r)
2   if  $r = \hat{q}$  then
3     | tensor_times_matrix(A, B, C, n, i, m, q, q̂,  $r - 1$ )
4   else if  $r > 1$  then
5     | for  $i_{\pi_r} \leftarrow 1$  to  $n_{\pi_r}$  do
6       | | tensor_times_matrix(A, B, C, n, i, m, q, q̂,  $r - 1$ )
7   else
8     | for  $j \leftarrow 1$  to  $m$  do
9       | | for  $i_q \leftarrow 1$  to  $n_q$  do
10        | | | for  $i_{\pi_1} \leftarrow 1$  to  $n_{\pi_1}$  do
11          | | | | C( $i_1, \dots, i_{q-1}, j, i_{q+1}, \dots, i_p$ ) += A( $i_1, \dots, i_q, \dots, i_p$ ) · B( $j, i_q$ )

```

Algorithm 1: Modified baseline algorithm with contiguous memory access for the tensor-matrix multiplication. The tensor order must be greater than one and for the contraction mode $1 \leq q \leq p$ and $\pi_1 \neq q$ must hold. The algorithm needs to be initially called with $r = p$ where \mathbf{n} is the shape tuple of $\underline{\mathbf{A}}$ and m is the q -th dimension of $\underline{\mathbf{C}}$.

205 limitation on tensor order and contraction mode. The arguments of `gemm` are
 206 chosen depending on the tensor order p , tensor layout π and contraction mode
 207 q except for the `CBLAS_ORDER` which is `CblasRowMajor`. The following description
 208 can be used to also define eight cases for the `CblasColMajor` format. You can find
 209 the parameter arguments in our C++ library.

210 *Case 1* ($p = 1$): The tensor-vector product $\underline{\mathbf{A}} \times_1 \mathbf{B}$ can be computed with a
 211 `gemv` operation $\mathbf{a}^T \cdot \mathbf{B}$ where $\underline{\mathbf{A}}$ is an order-1 tensor, i.e. a vector \mathbf{a} of length n_1 .

212 *Case 2-5* ($p = 2$): If $\underline{\mathbf{A}}$ and $\underline{\mathbf{C}}$ are order-2 tensors, i.e. a matrix \mathbf{A} with
 213 dimensions n_1 and n_2 , then a single `gemm` suffices to compute the tensor-matrix
 214 product. If \mathbf{A} and \mathbf{C} have the column-major format with $\pi = (1, 2)$, `gemm` either
 215 executes $\mathbf{C} = \mathbf{A} \cdot \mathbf{B}^T$ for $q = 1$ or $\mathbf{C} = \mathbf{B} \cdot \mathbf{A}$ for $q = 2$. Note that `gemm` interprets
 216 \mathbf{C} and \mathbf{A} as matrices using the reshaping operation ρ with $\rho = (2, 1)$ in row-
 217 major format even though both are stored column-wise. If \mathbf{A} and \mathbf{C} have the
 218 row-major format with $\pi = (2, 1)$, `gemm` either executes $\mathbf{C} = \mathbf{B} \cdot \mathbf{A}$ for $q = 1$ or
 219 $\mathbf{C} = \mathbf{A} \cdot \mathbf{B}^T$ for $q = 2$. The transposition of \mathbf{B} is necessary for the cases 2,5 and
 220 independent of the chosen storage format.

221 *Case 6-7* ($p > 2$): If the order of $\underline{\mathbf{A}}$ and $\underline{\mathbf{C}}$ is greater than 2 and if the
 222 contraction mode q is equal to π_1 (case 6), a single `gemm` with the depicted
 223 arguments executes $\mathbf{C} = \mathbf{A} \cdot \mathbf{B}^T$ and computes a tensor-matrix product $\underline{\mathbf{C}} =$
 224 $\underline{\mathbf{A}} \times_{\pi_1} \mathbf{B}$ for any storage layout of $\underline{\mathbf{A}}$ and $\underline{\mathbf{C}}$. Tensors $\underline{\mathbf{A}}$ and $\underline{\mathbf{C}}$ are flattened with
 225 $\varphi_{2,p}$ to row-major matrices \mathbf{A} and \mathbf{C} . Matrix \mathbf{A} has $\tilde{n}_{\pi_1} = \tilde{n}/n_{\pi_1}$ rows and n_{π_1}
 226 columns while matrix \mathbf{C} has the same number of rows and m columns. If $\pi_p = q$
 227 (case 7), Tensors $\underline{\mathbf{A}}$ and $\underline{\mathbf{C}}$ are flattened with $\varphi_{1,p-1}$ to column-major matrices
 228 \mathbf{A} and \mathbf{C} . Matrix \mathbf{A} has n_{π_p} rows and $\tilde{n}_{\pi_p} = \tilde{n}/n_{\pi_p}$ columns while matrix \mathbf{C}
 229 has m rows and the same number of columns. A single `gemm` executes $\mathbf{C} = \mathbf{B} \cdot \mathbf{A}$

Case	Order p	Layout π	Mode q	Routine	T	M	N	K	A	LDA	B	LDB	LDC
1	1	-	1	gemv	-	m	n_1	-	B	n_1	<u>A</u>	-	-
2	2	(1, 2)	1	gemm	B	n_2	m	n_1	<u>A</u>	n_1	B	n_1	m
3	2	(1, 2)	2	gemm	-	m	n_1	n_2	B	n_2	<u>A</u>	n_1	n_1
4	2	(2, 1)	1	gemm	-	m	n_2	n_1	B	n_1	<u>A</u>	n_2	n_2
5	2	(2, 1)	2	gemm	B	n_1	m	n_2	<u>A</u>	n_2	B	n_2	m
6	> 2	any	π_1	gemm	B	\bar{n}_q	m	n_q	<u>A</u>	n_q	B	n_q	m
7	> 2	any	π_p	gemm	-	m	\bar{n}_q	n_q	B	n_q	<u>A</u>	\bar{n}_q	\bar{n}_q
8	> 2	any	π_2, \dots, π_{p-1}	gemm*	-	m	n_{π_1}	n_q	B	n_q	<u>A</u>	w_q	w_q

Table 1. Eight cases with **gemv** and **gemm** for the mode- q tensor-matrix multiplication. Arguments T, M, N, etc. of the BLAS are chosen with respect to the tensor order p , layout π and contraction mode q where T specifies if **B** is transposed. **gemm*** denotes multiple **gemm** calls with different tensor slices. Argument \bar{n}_q for case 6 and 7 is given by $\bar{n}_q = 1/n_q \prod_{r=1}^p n_r$. Matrix **B** has the row-major format.

and computes the tensor-matrix product $\underline{\mathbf{C}} = \underline{\mathbf{A}} \times_{\pi_p} \mathbf{B}$ for any storage layout of **A** and **C**. Note that in all cases no copy operation is performed in order to compute the desired contraction, see subsection 3.

Case 8 ($p > 2$): If the tensor order is greater than 2 with $\pi_1 \neq q$ and $\pi_p \neq q$, the modified baseline algorithm 1 is used to successively call $\bar{n}/(n_q \cdot n_{\pi_1})$ times **gemm** with different tensor slices of **C** and **A**. Each **gemm** computes one slice $\underline{\mathbf{C}}'_{\pi_1, q}$ of the tensor-matrix product **C** using the corresponding tensor slices $\underline{\mathbf{A}}'_{\pi_1, q}$ and the matrix **B**. The matrix-matrix product $\mathbf{C} = \mathbf{B} \cdot \mathbf{A}$ is performed by interpreting both tensor slices as row-major matrices **A** and **C** which have the dimensions (n_q, n_{π_1}) and (m, n_{π_1}) , respectively. Please note that Algorithm 2 in [7] suggests to transpose matrix **B**.

4.3 BLAS-Based Algorithms with Subtensors

Case 8 can be optimized by utilizing larger subtensors instead of tensor slices. This can be accomplished by adding mergeable modes to the slice-matrix multiplication in which the subtensor can be flattened into a matrix without reordering tensor elements, see lemma 4.1 in [7]. We will use our flattening operation which does not copy or reorder elements, see section 3. The number of mergeable modes is $\hat{q}-1$ with $\hat{q} = \pi^{-1}(q)$ and the corresponding modes are $\pi_1, \pi_2, \dots, \pi_{\hat{q}-1}$. Applying flattening $\varphi_{1, q-1}$ and reshaping ρ with $\rho = (2, 1)$ on a subtensor of **A** with dimensions $n_{\pi_1}, \dots, n_{\pi_{\hat{q}-1}}, n_q$ yields a row-major matrix **A** with shape $(n_q, \prod_{r=1}^{\hat{q}-1} n_{\pi_r})$. Analogously, tensor **C** becomes a row-major matrix with the shape $(m, \prod_{r=1}^{\hat{q}-1} n_{\pi_r})$. This description supports all linear tensor layouts and generalizes lemma 4.2 in [7].

Algorithm 1 needs a minor modification so that **gemm** can be used with flattened subtensors instead of tensor slices. The modified algorithm therefor iterates only over modes larger than \hat{q} in the non-base case and hence omits the

first \hat{q} modes $\pi_{1,\hat{q}} = (\pi_1, \dots, \pi_{\hat{q}})$ with $\pi_{\hat{q}} = q$. The conditions in line 2 and 4 are changed to $1 < r \leq \hat{q}$ and $\hat{q} < r$, respectively. The single indices of the subtensors $\underline{\mathbf{A}}'_{\pi_{1,\hat{q}}}$ and $\underline{\mathbf{C}}'_{\pi_{1,\hat{q}}}$ are given by the loop induction variables that belong to the π_r -th loop with $\hat{q} + 1 \leq r \leq p$.

4.4 Parallel BLAS-based Algorithms

The following paragraphs discuss three parallel approaches for the eighth case. Cases 1 to 7 already call a multi-threaded `gemm`.

Sequential Loops and Multithreaded Matrix Multiplication A simple approach is to leave algorithm 1 unmodified and sequentially call a multi-threaded `gemm` in the base case as described in subsection 4.2. This is beneficial if $q = \pi_{p-1}$, if the inner dimensions n_{π_1}, \dots, n_q are large or if the outer-most dimension n_{π_p} is smaller than the available processor cores. However, if the above conditions are not met, the processor cores might not be fully utilized where each multi-threaded `gemm` is executed with small subtensors. We will refer to this algorithm version as `<seq-loops,par-gemm>` that is executable with subtensors or tensor slices.

Parallel Loops and Single or Multithreaded Matrix Multiplication A more advanced version of the above algorithm executes a single-threaded `gemm` in parallel with all available (free) modes. The number of free modes depends on the tensor slicing. If subtensors are used, all $\pi_{\hat{q}+1}, \dots, \pi_p$ modes are free and can be used for parallel execution. In case of tensor slices, only π_1 and $\pi_{\hat{q}}$ are free modes. The corresponding maximum degree of parallelism for both cases is $\prod_{r=\hat{q}+1}^p n_{\pi_r}$ and $\prod_{r=1}^p n_r / (n_{\pi_1} n_{\pi_{\hat{q}}})$, respectively.

Using tensor slices for the multiplication, $\underline{\mathbf{A}}$ and $\underline{\mathbf{C}}$ are flattened twice with $\varphi_{\pi_{\hat{q}+1}, \pi_p}$ and $\varphi_{\pi_2, \pi_{\hat{q}-1}}$. The resulting tensor is of order 4 with dimensions $n_{\pi_1}, \hat{n}_{\pi_2}, n_q, \hat{n}_{\pi_4}$ where $\hat{n}_{\pi_2} = \prod_{r=2}^{\hat{q}-1} n_{\pi_r}$ and $\hat{n}_{\pi_4} = \prod_{r=\hat{q}+1}^p n_{\pi_r}$. In this way the tree-recursion has been transformed in two loops. The outer loop iterates over \hat{n}_{π_4} while the inner loop iterates over \hat{n}_{π_2} calling `gemm` with slices $\underline{\mathbf{A}}'_{\pi_1, q}$ and $\underline{\mathbf{C}}'_{\pi_1, q}$. Both loops are parallelized using `omp parallel for` together with the `collapse(2)` and the `num_threads` clause which specifies the thread number.

In case of the general subtensor-matrix approach, both tensors are flattened twice with $\varphi_{\pi_{\hat{q}+1}, \pi_p}$ and $\varphi_{\pi_1, \pi_{\hat{q}-1}}$. The resulting tensor is of order 3 with dimensions $\hat{n}_{\pi_1}, n_q, \hat{n}_{\pi_4}$ where $\hat{n}_{\pi_1} = \prod_{r=1}^{\hat{q}-1} n_{\pi_r}$ and $\hat{n}_{\pi_4} = \prod_{r=\hat{q}+1}^p n_{\pi_r}$. The corresponding algorithm consists of one loops which iterates over \hat{n}_{π_4} calling single-threaded `gemm` with multiple subtensors $\underline{\mathbf{A}}'_{\pi', q}$ and $\underline{\mathbf{C}}'_{\pi', q}$ with $\pi' = (\pi_1, \dots, \pi_{\hat{q}-1})$.

Both algorithm variants will be referred to as `<par-loops,seq-gemm>` which can be used with subtensors or tensor slices. Note that `<seq-loops,par-gemm>` and `<par-loops,seq-gemm>` are opposing versions where either `gemm` or the free loops are performed in parallel. The all-parallel version `<par-loops,par-gemm>` executes available loops in parallel where each loop thread executes a multi-threaded `gemm` with either subtensors or tensor slices.

297 **Multithreaded batched Matrix Multiplication** The next version of the
 298 base algorithm is a modified version of the general subtensor-matrix approach
 299 that calls a single batched `gemm` for the eighth case. The subtensor dimensions
 300 and remaining `gemm` arguments remain the same. The library implementation is
 301 responsible how subtensor-matrix multiplications are executed and if subtensors
 302 are further divided into smaller subtensors or tensor slices. This version will be
 303 referred to as the `<gemm_batch>` variant.

304 5 Experimental Setup

305 **Computing System** The experiments have been carried out on an Intel Xeon
 306 Gold 6248R processor with a Cascade micro-architecture. The processor consists
 307 of 24 cores operating at a base frequency of 3 GHz. With 24 cores and a peak
 308 AVX-512 boost frequency of 2.5 GHz, the processor achieves a theoretical data
 309 throughput of ca. 1.92 double precision Tflops. We measured a peak performance
 310 of 1.78 double precision Tflops using the likwid performance tool.

311 We have used the GNU compiler v10.2 with the highest optimization level `-O3`
 312 and `-march=native`, `-pthread` and `-fopenmp`. Loops within for the eighth case have
 313 been parallelized using GCC’s OpenMP v4.5 implementation. We have used the
 314 `gemv` and `gemm` implementation of the 2024.0 Intel MKL and its own threading
 315 library `mkl_intel_thread` together with the threading runtime library `libiomp5`.

316 If not otherwise mentioned, both tensors $\underline{\mathbf{A}}$ and $\underline{\mathbf{C}}$ are stored according to
 317 the first-order linear tensor layout with $\pi = (1, \dots, p)$ whereas matrix \mathbf{B} has the
 318 row-major storage format.

319 **Tensor Shapes** We have used asymmetrically and symmetrically shaped ten-
 320 sors in order to cover many use cases. The dimension tuples of both shape types
 321 are organized within two three-dimensional arrays with which tensors are ini-
 322 tialized. The dimension array for the first shape type contains $720 = 9 \times 8 \times 10$
 323 dimension tuples where the row number is the tensor order ranging from 2 to
 324 10. For each tensor order, 8 tensor instances with increasing tensor size is gen-
 325 erated. A special feature of this test set is that the contraction dimension and
 326 the leading dimension are disproportionately large. The second set consists of
 327 $336 = 6 \times 8 \times 7$ dimensions tuples where the tensor order ranges from 2 to 7 and
 328 has 8 dimension tuples for each order. Each tensor dimension within the second
 329 set is 2^{12} , 2^8 , 2^6 , 2^5 , 2^4 and 2^3 . A detailed explanation of the tensor shape setup
 330 is given in [2, 3].

331 6 Results and Discussion

332 **Slicing Methods** The next paragraphs analyze the two proposed slicing meth-
 333 ods and discuss runtime results of `<par-loops,seq-gemm>` and `<gemm_batch>` using
 334 asymmetrically and symmetrically shaped tensors. Fig. 1 contains six contour
 335 plots (performance maps) in which `<par-loops,seq-gemm>` either uses subtensors
 336 or tensor slices and `<gemm_batch>` loops over subtensors only. Each point within

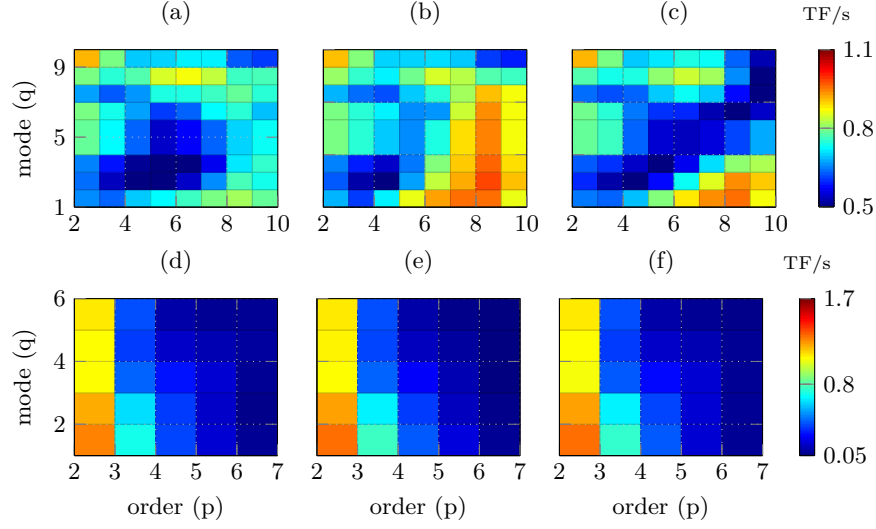


Fig. 1. Performance maps in double-precision Tflops of the proposed algorithms with varying tensor orders p and contraction modes q . Tensors are asymmetrically shaped on the top plots and symmetrically shaped on the bottom plots. In (a) and (d) function `<gemm_batch>` is executed, in (b) and (e) `<par-loops,seq-gemm>` with tensor slices, in (c) and (f) `<par-loops,seq-gemm>` with subtensors.

the performance map represents a mean value that has been averaged over tensor sizes for a tensor order¹.

For asymmetrically shaped tensors, function `<par-loops,seq-gemm>` with tensor slices performs on average 18% better than with subtensors and is on average 11% faster than Intel’s `gemm_batch` routine. It reaches almost 1.1 Tflops for non-edge cases with $q > 2$ and $p > 6$. This suggests that the Intel’s implementation does not divide subtensors into smaller blocks.

With symmetrically shaped tensors, `<par-loops,seq-gemm>` with tensor slices and `<gemm_batch>` perform almost equally well and reach 221.52 Gflops and 236.21 Gflops, respectively. Moreover, the slicing method seems to have only little affect on the overall runtime behavior of `<par-loops,seq-gemm>`. In contrast to the performance maps with asymmetrically shaped tensors, all functions almost reach the attainable peak performance of 1.7 Tflops when $p = 2$. This can be by the fact that both dimensions are equal or larger than 4096 enabling `gemm` to operate under optimal conditions.

Parallelization Methods The contour plots in Fig. 1 contain performance data of all cases except for 4 and 5, see Table 1. The effects of the presented slicing and parallelization methods can be better understood if performance data of only

¹ Note that Fig. 2 suggests that the contraction mode q can be greater than p which is not possible. Our profiling program sets $q = p$ in such cases.

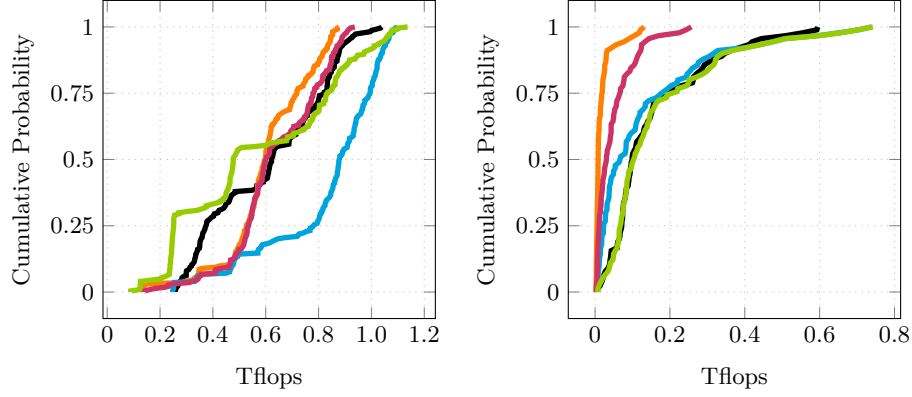


Fig. 2. Cumulative performance distributions of the proposed algorithms for the eighth case. Each distribution line belongs to one algorithm: `<gemm_batch>` (black), `<seq-loops,par-gemm>` (orange) and `<par-loops,seq-gemm>` (blue) using tensor slices, `<seq-loops,par-gemm>` (pink) and `<par-loops,seq-gemm>` (green) using subtenors. Tensors are asymmetrically (left plot) and symmetrically shaped (right plot).

the eighth case is examined. Fig. 2 contains cumulative performance distributions of all the proposed algorithms which are generated `gemm` or `gemm_batch` calls within case 8. As the distribution is empirically computed, the probability y of a point (x, y) on a distribution function corresponds to the number of test cases of a particular algorithm that achieves x or less Tflops. For instance, function `<seq-loops,par-gemm>` with subtenors computes the tensor-matrix product for 50% percent of the test cases with equal to or less than 0.6 Tflops in case of asymmetrically shaped tensor. Consequently, distribution functions with an exponential growth are favorable while logarithmic behavior is less desirable. The test set cardinality for case 8 is 255 for asymmetrically shaped tensors and 91 for symmetrically ones.

In case of asymmetrically shaped tensors, `<par-loops,seq-gemm>` with tensor slices performs best and outperforms `<gemm_batch>`. One unexpected finding is that function `<seq-loops,par-gemm>` with any slicing strategy performs better than `<gemm_batch>` when the tensor order p and contraction mode q satisfy $4 \leq p \leq 7$ and $2 \leq q \leq 4$, respectively. Functions executed with symmetrically shaped tensors reach at most 743 Gflops for the eighth case which is less than half of the attainable peak performance of 1.7 Tflops. This is expected as cases 2 and 3 are not considered. Functions `<par-loops,seq-gemm>` with subtenors and `<gemm_batch>` have almost the same performance distribution outperforming `<seq-loops,par-gemm>` for almost every test case. Function `<par-loops,seq-gemm>` with tensor slices is on average almost as fast as with subtenors. However, if the tensor order is greater than 3 and the tensor dimensions are less than 64, its running time increases by almost a factor of 2.

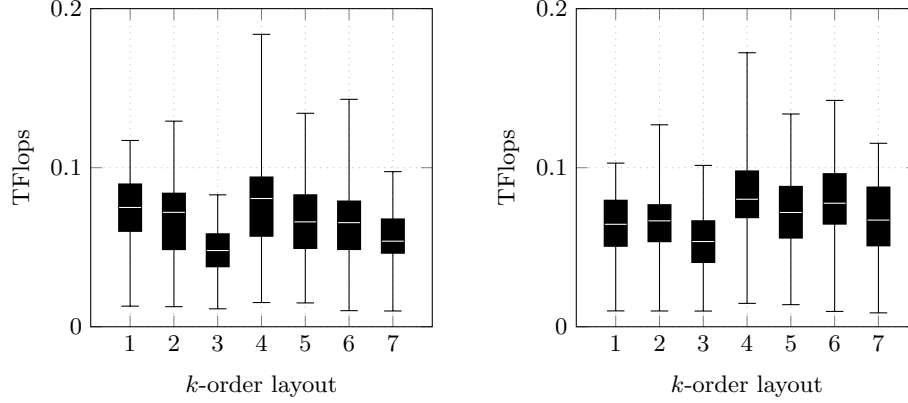


Fig. 3. Box plots visualizing performance statistics in double-precision Tflops of `<gemm_batch>` (left) and `<par-loops, seq-gemm>` with subtenors (right). Box plot number k denotes the k -order tensor layout of symmetrically shaped tensors with order 7.

These observations suggest to use `<par-loops, seq-gemm>` with tensor slices for common cases in which the leading and contraction dimensions are larger than 64 elements. Subtenors should only be used if the leading dimension n_{π_1} of $\underline{\mathbf{A}}_{\pi_1, q}$ and $\underline{\mathbf{C}}_{\pi_1, q}$ falls below 64. This strategy is different to the one presented in [7] that maximizes the number of modes involved in the matrix multiply. We have also observed no performance improvement if `par-gemm` was used with `par-loops` which is why their distribution functions are not shown in Fig. 2. Moreover, in most cases the `seq-loops` implementations are independent of the tensor shape slower than `par-loops`, even for smaller tensor slices.

Layout-Oblivious Algorithms Fig. 3 contains two subfigures visualizing performance statistics in double-precision Tflops of `<gemm_batch>` (left subfigure) and `<par-loops, seq-gemm>` with subtenors (right subfigure). Each box plot with the number k has been computed from benchmark data with symmetrically shaped order-7 tensors with the k -order tensor layout. The 1-order and 7-order layout, for instance, are the first- and last-order storage formats for the order-7 tensor with $\pi_F = (1, 2, \dots, 7)$ and $\pi_L = (7, 6, \dots, 1)$. The definition of k -order tensor layouts can be found in section 3.

The low performance of around 70 Gflops can be attributed to the fact that the contraction dimension of subtenors of tensor slices of symmetrically shaped order-7 tensors are 8 while the leading dimension is 8 or at most 48 for subtenors. The relative standard deviation of `<gemm_batch>`'s and `<par-loops, seq-gemm>`'s median values are 12.95% and 17.61%. Their respective interquartile range are similar with a relative standard deviation of 22.25% and 15.23%.

The runtime results with different k -order tensor layouts show that the performance of our proposed algorithms is not designed for a specific tensor layout. Moreover, the performance stays within an acceptable range independent of the tensor layout.

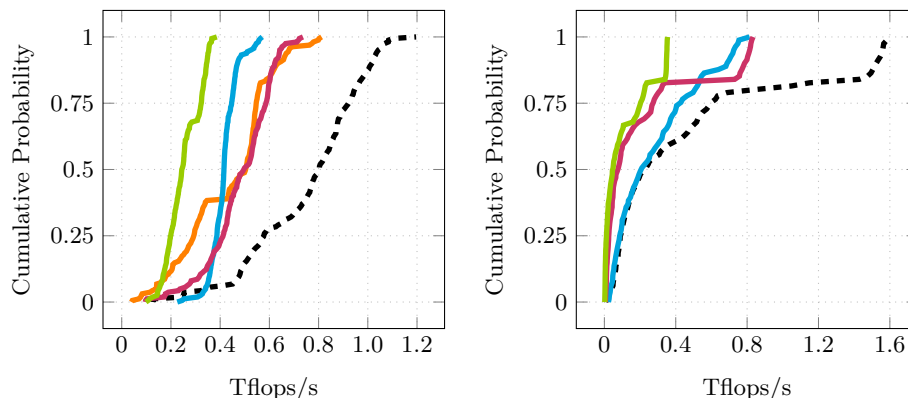


Fig. 4. Cumulative performance distributions of tensor-times-matrix algorithms in double-precision Tflops. Each distribution line belongs to a library: **tlib**[ours] (---), **tcl** (—), **tblis** (—), **libtorch** (—), **eigen** (—). Libraries have been tested with asymmetrically-shaped (left plot) and symmetrically-shaped tensors (right plot).

Comparison with other Approaches We have compared our best implementation with four libraries that implement the tensor-matrix multiplication using different approaches. Library **tcl** implements the TTGT approach with a high-perform tensor-transpose library **hptt** which is discussed in [16]. **tblis** implements the GETT approach that is akin to Blis’ algorithm design for the matrix multiplication [9]. The tensor extension of **eigen** (v3.3.7) is used by the Tensorflow framework. Library **libtorch** (v2.3.0) is the C++ distribution of PyTorch. **tlib** denotes our library using algorithm `<par-loops,seq-gemm>` that have been presented in the previous paragraphs.

Fig. 2 contains cumulative performance distributions for the complete test sets comparing the performance distribution of our implementation with the previously mentioned libraries. Note that we only have used tensor slices for asymmetrically shaped tensors (left plot) and subtensors for symmetrically shaped tensors (right plot). Our implementation with a median performance of 793.75 Gflops outperforms others’ for almost every asymmetrically shaped tensor in the test set. The median performances of **tcl**, **tblis**, **libtorch** and **eigen** are 503.61, 415.33, 496.22 and 244.69 Gflops reaching on average 74.11%, 61.14%, 76.68% and 39.34% of **tlib**’s throughputs.

In case of symmetrically shaped tensors the performance distributions of all libraries on the right plot in Fig. 2 are much closer. The median performances of **tlib**, **tblis**, **libtorch** and **eigen** are 228.93, 208.69, 76.46, 46.25 Gflops reaching on average 73.06%, 38.89%, 19.79% of **tlib**’s throughputs². All libraries operate with 801.68 or less Gflops for the cases 2 and 3 which is almost half of **tlib**’s performance with 1579 Gflops. The median performance and the interquartile

² We were unable to run **tcl** with our test set containing symmetrically shaped tensors. We suspect a very high memory demand to be the reason.

range of **tblis** and **tlib** for the cases 6 and 7 are almost the same. Their respective median Gflops are 255.23 and 263.94 for the sixth case and 121.17 and 144.27 for the seventh case. This explains the similar performance distributions when their performance is less than 400 Gflops. **Libtorch** and **eigen** compute the tensor-matrix product, in median, with 17.11 and 9.64 Gflops/s, respectively. Our library **tlib** has a median performance of 102.11 Gflops and outperforms **tblis** with 79.35 Gflops for the eighth case.

7 Conclusion and Future Work

We presented efficient layout-oblivious algorithms for the compute-bound tensor-matrix multiplication which is essential for many tensor methods. Our approach is based on the LOG-method and computes the tensor-matrix product in-place without transposing tensors. It applies the flexible approach described in [2] and generalizes the findings on tensor slicing in [7] for linear tensor layouts. The resulting algorithms are able to process dense tensors with arbitrary tensor order, dimensions and with any linear tensor layout all of which can be runtime variable.

Our benchmarks show that dividing the base algorithm into eight different GEMM cases improves the overall performance. We have demonstrated that algorithms with parallel loops over single-threaded GEMM calls with tensor slices and subtensors perform best. Interestingly, they outperform a single batched GEMM with subtensors, on average, by 14% in case of asymmetrically shaped tensors and if tensor slices are used. Both version computes the tensor-matrix product on average faster than other state-of-the-art implementations. We have shown that our algorithms are layout-oblivious and do not need further refinement if the tensor layout is changed. We measured a relative standard deviation of 12.95% and 17.61% with symmetrically-shaped tensors for different k -order tensor layouts.

One can conclude that LOG-based tensor-times-matrix algorithms are on par or can even outperform TTGT-based and GETT-based implementations without losing their flexibility. Hence, other actively developed libraries such as LibTorch and Eigen might benefit from implementing the proposed algorithms. Our header-only library provides C++ interfaces and a python module which allows frameworks to easily integrate our library.

In the future, we intend to generalize LOG-based approach for general tensor contractions with the same flexibility that we offered for the tensor-matrix multiplication. We would like to further optimize the tensor-matrix multiplication based on benchmark results of matrix-matrix products which might lead to better runtime results for edge cases.

Source Code Availability Project description and source code can be found at <https://github.com/bassoy/ttm>. The sequential tensor-matrix multiplication of TLIB is part of uBLAS and in the official release of **Boost v1.70.0** and later.

References

1. Bader, B.W., Kolda, T.G.: Algorithm 862: Matlab tensor classes for fast algorithm prototyping. *ACM Trans. Math. Softw.* **32**, 635–653 (December 2006)
2. Basso, C.: Design of a high-performance tensor-vector multiplication with blas. In: *International Conference on Computational Science*. pp. 32–45. Springer (2019)
3. Basso, C., Schatz, V.: Fast higher-order functions for tensor calculus with tensors and subtensors. In: *International Conference on Computational Science*. pp. 639–652. Springer (2018)
4. Karahan, E., Rojas-López, P.A., Bringas-Vega, M.L., Valdés-Hernández, P.A., Valdes-Sosa, P.A.: Tensor analysis and fusion of multimodal brain images. *Proceedings of the IEEE* **103**(9), 1531–1559 (2015)
5. Kolda, T.G., Bader, B.W.: Tensor decompositions and applications. *SIAM review* **51**(3), 455–500 (2009)
6. Lee, N., Cichocki, A.: Fundamental tensor operations for large-scale data analysis using tensor network formats. *Multidimensional Systems and Signal Processing* **29**(3), 921–960 (2018)
7. Li, J., Battaglino, C., Perros, I., Sun, J., Vuduc, R.: An input-adaptive and in-place approach to dense tensor-times-matrix multiply. In: *High Performance Computing, Networking, Storage and Analysis*, 2015. pp. 1–12. IEEE (2015)
8. Lim, L.H.: Tensors and hypermatrices. In: Hogben, L. (ed.) *Handbook of Linear Algebra*. Chapman and Hall, 2 edn. (2017)
9. Matthews, D.A.: High-performance tensor contraction without transposition. *SIAM Journal on Scientific Computing* **40**(1), C1–C24 (2018)
10. Napoli, E.D., Fabregat-Traver, D., Quintana-Ortí, G., Bientinesi, P.: Towards an efficient use of the blas library for multilinear tensor contractions. *Applied Mathematics and Computation* **235**, 454 – 468 (2014)
11. Papalexakis, E.E., Faloutsos, C., Sidiropoulos, N.D.: Tensors for data mining and data fusion: Models, applications, and scalable algorithms. *ACM Transactions on Intelligent Systems and Technology (TIST)* **8**(2), 16 (2017)
12. Paszke, A., Gross, S., Massa, F., Lerer, A., Bradbury, J., Chanan, G., Killeen, T., Lin, Z., Gimelshein, N., Antiga, L., et al.: Pytorch: An imperative style, high-performance deep learning library. *Advances in neural information processing systems* **32** (2019)
13. Pawlowski, F., Uçar, B., Yzelman, A.J.: A multi-dimensional morton-ordered block storage for mode-oblivious tensor computations. *Journal of Computational Science* **33**, 34–44 (2019)
14. Shi, Y., Niranjana, U.N., Anandkumar, A., Cecka, C.: Tensor contractions with extended blas kernels on cpu and gpu. In: *2016 IEEE 23rd International Conference on High Performance Computing (HiPC)*. pp. 193–202 (Dec 2016)
15. Solomonik, E., Matthews, D., Hammond, J., Demmel, J.: Cyclops tensor framework: Reducing communication and eliminating load imbalance in massively parallel contractions. In: *Parallel & Distributed Processing (IPDPS), 2013 IEEE 27th International Symposium on*. pp. 813–824. IEEE (2013)
16. Springer, P., Bientinesi, P.: Design of a high-performance gemm-like tensor-tensor multiplication. *ACM Transactions on Mathematical Software (TOMS)* **44**(3), 28 (2018)